Humidity and polarity influence on MIM PZT capacitor degradation and breakdown

Jiahui Wang, Cora Salm, Evert Houwman, Minh Nguyen, Jurriaan Schmitz
MESA+ Institute for Nanotechnology, University of Twente, 7500 AE Enschede, the Netherlands.

***Abstract*—This paper presents a reliability study on unpackaged metal-PZT-metal capacitors. Both ramped voltage stress (RVS) and time dependent dielectric breakdown (TDDB) measurements show that environmental humidity dramatically worsens the PZT reliability. Visible breakdown spots on the surface of PZT capacitors are studied in detail. The measurement results indicate that both reversible and irreversible PZT degradation/breakdown happen during TDDB. The dependence of time to breakdown on polarity of applied voltage is argued to relate to the crystal structure of PZT and the stack of the PZT capacitor.**

Keywords—PZT; MEMS; TDDB; grain boundary; grain size; defects; degradation; breakdown; oxygen ion; oxygen vacancy

I. Introduction

$PbZr_{1-x}Ti_xO_3$ (PZT) exhibits excellent piezoelectric properties, exploited in many MEMS devices [1,2]. A prolonged exposure to high voltages is a prerequisite for the application of such devices in products. The reliability of the PZT thin film under electrical bias becomes a decisive factor in its commercialization [3-5].

To study the physics of PZT degradation and breakdown, we conduct ramped voltage stress (RVS) and time-dependent-dielectric-breakdown (TDDB) measurements on metal-insulator-metal (MIM) PZT capacitors with various stacks. In this paper, we present the influence of environmental humidity, the effect of electrodes and PZT microstructure on the TDDB behaviour of PZT MIM stacks.

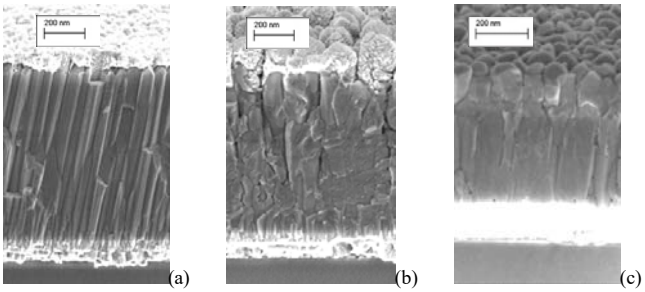

Figure 1 SEM cross-section views of MIM PZT capacitors with (a) Pt electrodes and columnar PZT grains, (b) Pt electrodes and dense PZT, (c) LNO electrodes.

II. Experiments

In this study, the PZT films are deposited on (111)/Pt/Ti/SiO_2/Si substrates using pulsed laser deposition (PLD). To prevent the formation of pyrochlore phase at the interface between PZT film and Pt bottom electrode, a thin layer of $LaNiO_3$ (LNO, 10 nm, using PLD) is inserted between Pt bottom and PZT film, as shown in Figs 1(a)-1(b). A layer of 90-nm-thick Pt is used as the top electrode. 120-nm-thick LNO layers are also used as electrodes of some PZT MIM capacitors under study, as in Fig. 1 (c). The PZT layer is 900 nm in Fig. 1 (a) and (b); and 350 nm in Fig. 1 (c). The top electrode size of all measured PZT capacitors is 100×100 μm^2. More details of the MIM PZT capacitor fabrication are found in [6].

A Keithley 4200 SCS and a probe station are used for all electrical measurements presented in this paper. The bottom electrodes of the capacitors are always grounded and the voltages are applied to the top electrodes. The current is measured from the top electrode. The current compliance is set to 100 nA for all TDDB measurements; this compliance level is also used as the breakdown criterion. All the measurements mentioned in this paper are wafer-level on unpackaged devices.

III. Results and analysis

A. *Influence of environmental humidity on PZT breakdown*

RVS measurements of the same MIM PZT capacitors (as in Fig. 1 (a)) are done under two relative humidity (RH) conditions. The leakage current of the PZT capacitor increases faster when the humidity is high, as shown in Fig. 2. During this stress condition, the surface of the PZT capacitor changes over time, namely spots appear as observed using an optical microscope. Under high humidity, these spots occur much more frequently under similar bias conditions as shown in the insets of Fig. 2.

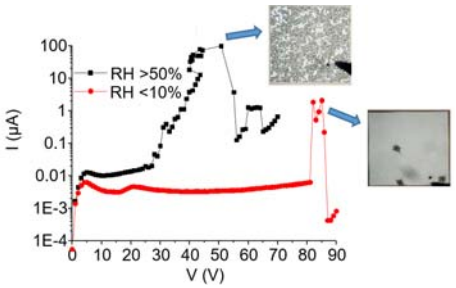

Figure 2 RVS measurements under two RH conditions. The insets are optical microscope photos of top electrodes of the measured capacitors at voltages marked by the arrows.

These breakdown spots on the top electrode are carefully observed by scanning electron microscopy (SEM), as shown in Fig. 3. The breakdown spots in both high and low RH have a similar structure. The outer edge of the breakdown spot is irregular. One (Fig. 3 (a)) or several (Fig. 3 (c)) holes are observed in the center of the spot. There are many spherical particles inside the holes. Comparing Fig. 3 (b) (RH<10%) and Fig. 3 (c) (RH>50%), the diameter of the holes in low RH (tens of micrometres) is much larger than that in high RH (several micrometres).

The elemental composition is measured at various positions on the broken surfaces by energy dispersive spectroscopy (EDS). In Fig. 3 (c), position *a* outside the breakdown spot is pure Pt. Position *b* between the central hole and the outer edge of the breakdown spot consists of PZT. Position *c*, one of the spheres inside the central hole, is Pt. At position *d* inside the central hole besides the spheres we find SiO_x. If we zoom in to see the area marked by the red square in Fig. 3 (c), the sidewall of the PZT layer appears as shown in Fig. 3 (d). Although inside the breakdown spot, the PZT columns are still structurally similar to the fresh PZT layer.

In short, we get the following information from SEM/EDS results. At the breakdown spot, the bottom electrode melts and recondensates in the form of spheres on the SiO_x substrate. Some PZT disappears, leading to holes in the PZT layer at the centre of the breakdown spots. The top electrode above and around the PZT holes also melts, resulting in the irregular outer edges of the breakdown spots.

We interpret the appearance of these breakdown spots as the result of local discharges (fed by the capacitive energy of the voltage biased MIM capacitor). The current is not uniformly distributed in the PZT capacitor. We assume that the current concentrates around weak points in the PZT. Given the high overall current that flows during the RVS measurement, the generated Joule heat is able to melt the weak points in the PZT and/or the electrode [7]. Defects are considered the main reason of non-uniformity of current in PZT capacitor [8-10]. J. S. Lee *et al*. show that the leakage current through grain boundaries is larger than that through PZT bulk. The increase of grain boundary density leads to a decrease of breakdown field [11]. The field-induced local dielectric breakdown or field-assisted emission of trapped charged carriers at grain boundaries are mentioned in the PZT degradation model summarized by Waser *et al*. [9]. Therefore, it possible that the defects accumulated at grain boundaries act as the weak points in PZT. Water molecules are likely to penetrate PZT along the grain boundaries, influencing these weak spots in the PZT material.

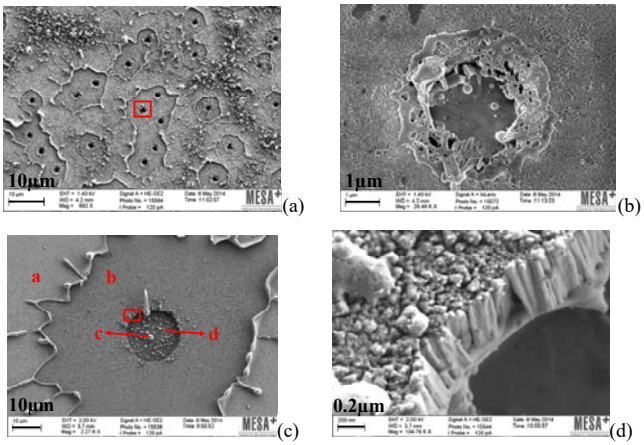

Figure 3 SEM micrographs of (a) breakdown spots corresponding to RVS measurement at RH>50% and (b) its zoom in image of the red square marked area; (c) one breakdown spot corresponding to RVS measurement at RH<10% and (d) its zoom in image of the red square marked area.

High environmental humidity also worsens TDDB behavior of MIM PZT capacitors. Fig. 4 shows the Weibull distribution of the same PZT capacitors (as in Fig. 1 (a)) under two humidity conditions. Compared with the TDDB result at low RH, the Weibull scale parameter is significantly decreased at high RH, which indicates a decrease of the breakdown time; the decrease of Weibull shape parameter under high RH indicates that high humidity increases the number of (active) defects in PZT and triggers breakdown [12].

All the above measurements indicate that high RH results in an increase of (active) defects in PZT. Indeed, when sufficient water is adsorbed and dissociated on the surface of PZT capacitors, significant defects could be generated to cause PZT degradation [13]. Exposure of PZT to water (or NaOH solution) by itself is reported not to degrade PZT [14]. In our experiments, the combined exposure to moisture with a high electric field stress does lead to PZT degradation. Therefore, the extra defects in high RH may relate with the atomic hydrogen (H) generated by electrolysis of water. Pt probably plays as a catalysis in dissociation to generate atom H [15].

Hydrogen may change PZT properties through incorporation, diffusion and reaction with PZT. Atomic H can diffuse freely into bulk PZT and as such does not influence its properties. However, the penetration of H can induce structural degradation in various ways [16,17]. Firstly, at PZT grain boundaries or at the electrode/PZT interface, atomic H can react with oxygen ions and generate oxygen vacancies and electrons, resulting in a decrease of resistivity. Secondly, atomic H is indirectly involved in the dissociation of oxygen in the PZT lattice, generating oxygen vacancies. Thirdly, atomic H may form molecular H_2 and induce the reduction of PZT. Metallic Pb is found at grain boundaries and electrode/PZT interface. Pb further diffuses to the electrode interface and causes PZT degradation. Fourthly, the ionization of H in the PZT lattice releases electrons and decreases PZT resistivity. Ionic H^+ could react with oxygen ions in the lattice and form polar hydroxyl bonds H-O, which acts as a fixed dipole and hinders the switching of PZT domains. Finally, molecular H_2 existing at the grain boundaries may lead to cracks/voids [16]. The hydrogen induced PZT degradation seems mainly to happen at grain boundaries according to the mechanisms mentioned above.

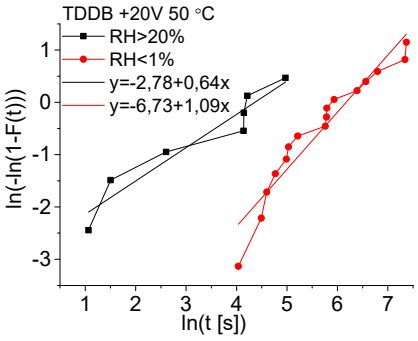

Figure 4 Weibull distribution for two RH conditions: the symbol lines are measurement results; the solid lines are linear fitting of the measurement results.

B. *TDDB: reversible and irreversible PZT degradation/breakdown*

To eliminate the influence of humidity, the MIM PZT capacitors are heated to 150 °C for 10 minutes with dry air flow before the TDDB measurement presented below; we keep the dry air flow on during TDDB to ensure RH<1%. The MIM PZT capacitor stacks treated in this section are as in Fig. 1 (a).

We find that the top electrodes of most PZT capacitors do not break (according to optical microscope inspection) during TDDB measurement. After removing the DC stress, the device recovers to the high resistivity state. When the recovery is complete, we repeat the TDDB measurement on the PZT capacitors which have no visible breakdown spots on the top electrodes. Typically, we store the PZT capacitors un-biased for several days between the two TDDB measurements to complete the PZT recovery. The current-time relation of one PZT capacitor during and between the first and second TDDB are shown in Fig. 5. The initial stress current at constant voltage during the second TDDB test is even smaller than that during the first TDDB.

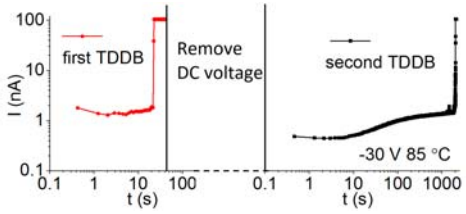

Figure 5 current-time relation during and between fist and second TDDB measurements of one PZT capacitor.

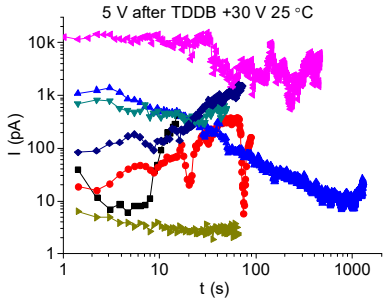

Figure 6 Current evolution of PZT capacitors at 5 V after first TDDB.

The PZT recovery process is detected by measuring the current after the first breakdown under a DC bias of 5 V (the polarity of this test voltage is the same as the polarity of the stress voltage used for TDDB). The current-time relation at 5 V is shown in Fig. 6. Most of the time, the leakage current decreases with time at 5 V, but with varying decrease rate. For some PZT capacitors, the leakage current even increases at 5 V. The top electrodes of the PZT capacitors mentioned here are not broken during TDDB. When the PZT capacitors stressed to first breakdown are un-biased for a long time, all of them will recover to the high resistivity state.

The Weibull distribution of the two TDDB measurements are shown in Fig. 7 (a). The time until second breakdown is always longer than the first TDDB time. We further note that the capacitance of the PZT capacitor decreases after the first TDDB; but does not further change after the second TDDB, as shown in Fig. 7 (b).

To understand these measurement results, it is necessary to distinguish degradation from breakdown. PZT degradation is a reversible process because of oxygen vacancy redistribution in PZT and barrier lowering at the electrode/PZT interface under a continuous voltage stress [8]. Usually, the PZT degradation does not change the dielectric properties of PZT, and the PZT film could recover to its initial state when the voltage stress is removed. The mechanism of PZT breakdown is not clear yet; it probably relates to defects in PZT [8]. Many mechanisms and models are proposed to explain PZT TDDB behavior, such as the percolation model [18], *E* model [19], infant mortality model [20] and electromigration model [21]. The observed TDDB behavior in this paper is reversible but cannot be explained by the published PZT degradation and relaxation theory [8], thus we think breakdown indeed happens during TDDB. It seems that the stress sequence of first TDDB disables some weak links in PZT; both reversible and irreversible PZT degradation/breakdown happen during TDDB.

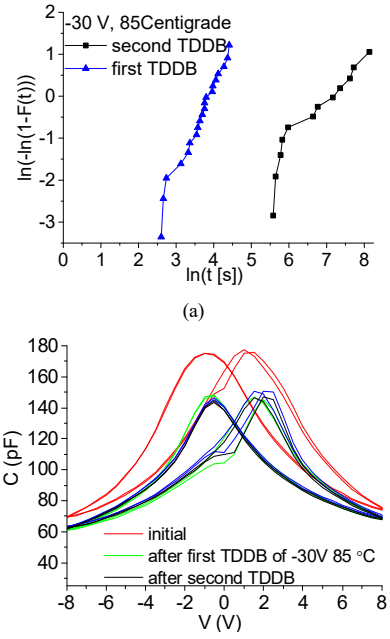

Figure 7 (a) the Weibull distribution of two subsequent TDDB measurements of the same PZT capacitors, (b) the capacitance-voltage relation of the fresh PZT capacitor, after the first TDDB, and after the second TDDB.

C. *Polarity influence and PZT microstructure*

When we apply DC voltages with opposite polarities but the same magnitude to the same PZT capacitors at RH<1%, we find a significant but nontrivial polarity dependence of the time to (first) breakdown, as shown in Fig. 8.

The dielectric breakdown process in PZT is probably a combination of electronic and thermal breakdown [8]. Since

the observed TDDB is reversible, we suppose that the migration of oxygen ions or vacancies contributes to TDDB by forming high conductivity paths for electrons. The continuous flow of electrons may heat PZT or induce trap generation in PZT, and finally triggers breakdown. The time to breakdown may relate with both the time to form the high conductivity path and the leakage current value.

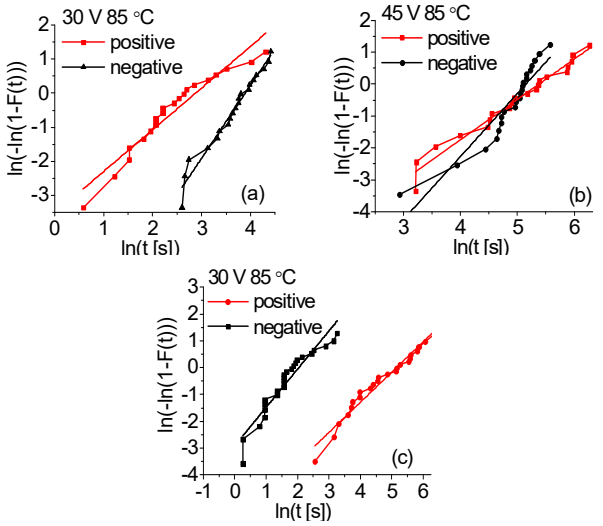

Figure 8 The Weibull distributions of positive/negative TDDB of three kinds of MIM PZT capacitors corresponding to figure 1 (a) (b) and (c).

For a PZT capacitor as in Fig. 1&8 (a), the negative-TDDB time is longer than the positive-TDDB time. When the top electrode is positively stressed, oxygen vacancies may move along the PZT grain boundaries to the bottom electrode, therefore, oxygen ions accumulate underneath the Pt top electrode, resulting in a reduction of the reverse-biased Schottky barrier (the un-doped PZT is p-type [6]). A high conductivity path is formed because of this redistribution of oxygen ions/vacancies. When the top electrode is negatively stressed, the oxygen ions accumulated near the bottom LNO-PZT interface are compensated by the oxygen vacancies in the LNO, so that the reverse-biased Schottky barrier is not reduced. Therefore, at negative voltage, it is relatively difficult to form the high conductivity path and to inject electrons, resulting in a long negative-TDDB time.

The TDDB results of PZT capacitors as Fig. 1&8 (b) are much better, as a higher voltage can be maintained across these capacitors with the same overall dimensions. Figure 8 (b) shows that the positive- and negative-TDDB times are more or less the same. The used materials and dimensions of Fig. 1 (a) and (b) are exactly the same. However, Fig. 1 (a) has PZT grain size of about 70 nm, and PZT grain columns connect the top and bottom electrodes. Fig. 1 (b) has dense PZT with grain sizes larger than 100 nm. Some PZT grain columns look merged together. No PZT grain boundaries directly connect the top and bottom electrode. It is possible that the PZT grain boundaries are the weakest links. Since no PZT grain boundaries, thus no high conductivity paths, connect the two electrodes in Fig. 1 (b), a positive stress on the top electrode does not trigger TDDB easier than negative stress.

As stated, a higher stress voltage is required to observe breakdown in Fig. 1 (b) than Fig. 1 (a). By changing the PLD parameters, we can get PZT with microstructure as Fig. 1 (b), but even smaller gap among PZT grains and more grains merged together. We find that the denser the PZT film is, the larger is the breakdown voltage. Yao *et al*. also point out that the dielectric strength is higher in denser and less rough microstructure PLD PZT [22]. Thus, the difference between Fig. 1 (a) and (b) should be explained by not only the PZT grain structure but also the PZT density.

For a PZT capacitor as Fig. 1&8 (c), the top LNO-PZT interface is rougher than the bottom LNO-PZT interface; and the columnar PZT grains connect the two electrodes. It can be expected that oxygen ions accumulate near the top LNO at positive stress; and accumulate near the bottom LNO at negative stress. Oxygen ions are apparently easier compensated near the rough top electrode than near the bottom electrode. Thus the result is opposite to Fig. 1&8 (a): positive-TDDB time is longer than negative-TDDB time.

IV. Conclusion

Humidity greatly worsens PZT degradation and breakdown. Both reversible and irreversible PZT degradation/breakdown are observed to happen during TDDB. After a first breakdown and recovery, a PZT capacitor will have a longer TDDB time; be it with a degraded overall capacitance. At the same composition and layer thickness, the crystal structure of PZT determines the breakdown voltage to a large extent. Closer HR-SEM inspection of more samples as Fig. 1 (b) leads to the suspicion that denser PZT samples reach higher breakdown voltages.

References

[1] S. Trolier-Mckinstry et al., J. Electroceramics, 12 (2004), 7-17.
[2] C. B. Eom et al., MRS Bulletin, 37 (2012), 1007-1017.
[3] H. Funakubo et al., MRS Bulletin, 37 (2012), 1030-1038.
[4] J. S. Pulskamp et al., MRS Bulletin, 37 (2012), 1062-1070.
[5] A. Mazzalai et al., J. Microelectromechanical Sys., 24 (2015), 831-838.
[6] M. D. Nguyen, PhD thesis of University of Twente, 2010.
[7] D. Zheng et al., Sensors and Actuators A, 241 (2016), 197–202.
[8] E. Defay, Ferroelectric Dielectrics Integrated on Silicon, Wiley, 2011.
[9] R. Waser et al., J. Am. Ceram. Soc., 73 (1990), 1645-1653.
[10] X. J. Meng et al., App. Phy. Lett., 78 (2001), 2548-2550.
[11] J. S. Lee et al., App. Phy. Lett., 81 (2002), 2602-2604.
[12] R. B. Abernethy, The new Weibull handbook, 2006.
[13] J. D. Baniecki, et al., App. Phy. Lett., 81 (2002), 3837-3839.
[14] W. P. Chen et al., App. Phy. Lett., 80 (2002), 3587-3589.
[15] C.K.Huang et al., J. App. Phy., 98 (2005), 104105(1-7).
[16] A. Shafiei J. App. Phy., 109 (2011), 114108(1-8).
[17] A. Shafiei et al., J. Materials Science, 49 (2013), 519-526.
[18] M. T. Chentir et al., Microelectronics Reliability, 49 (2009), 1074-1078.
[19] E. Bouyssoe et al., Integrated Ferroelectronics, 73 (2005), 49-56.
[20] J. S. Lee et al., Sensors and Actuators A, 154 (2009), 97-102.
[21] P. M. Weaver et al., Smart Material and Structure, 21 (2012), 1-9.
[22] Y. Yao et al., J. App. Phy., 95 (2004), 6341-6346.